magnetochemistry

Article

Bandwidth Enhancement of a Mobile Phone Antenna Using Ferrite Slab

Peng Li [1], Wei-Hua Zong [2,*], Zhejun Jin [2], Zhiqun Yang [3], Xiaoyun Qu [3] and Shandong Li [2,*]

1 College of Physics, Qingdao University, Qingdao 266071, China
2 School of Electronics and Information, Qingdao University, Qingdao 266071, China
3 Shandong Institute of Space Electronic Technology, Yantai 264003, China
* Correspondence: zongweihua@qdu.edu.cn (W.-H.Z.); lishd@qdu.edu.cn (S.L.)

Abstract: A novel technique to enhance the bandwidth of mobile phone antennas using YIG ferrite is proposed. The technique is applied in two slot antennas which are the proposed antenna and the reference antenna. The two antennas have the same shaped slot consisting of a rectangle connected to a circle etched on the ground plane. A ferrite slab is attached at the region near the circular slot on the ground plane of each antenna. The measured bandwidth of the proposed antenna with ferrite slab is enhanced to 0.669–1.533 and 1.69–5 GHz compared with the bandwidth of 0.81–1.44 and 2.3–5 GHz for the antenna without ferrite. The bandwidth of the reference antenna with ferrite slab is enhanced to 0.715–5 GHz compared with the bandwidth of 0.813–1.01, 1.11–1.3 and 2.33–5 GHz for the antenna without ferrite loading. The technique has the virtues of easy fabrication and low cost.

Keywords: antennas; ferrite; mobile phone antennas; slot antennas

Citation: Li, P.; Zong, W.-H.; Jin, Z.; Yang, Z.; Qu, X.; Li, S. Bandwidth Enhancement of a Mobile Phone Antenna Using Ferrite Slab. *Magnetochemistry* **2022**, *8*, 141. https://doi.org/10.3390/magnetochemistry8110141

Academic Editor: Zheng Gai

Received: 20 August 2022
Accepted: 20 October 2022
Published: 26 October 2022

1. Introduction

Ferrite and ferrite-based composite materials have properties of magnetic anisotropy, tunable permeability, high permittivity and permeability, which makes them good candidates for varieties of applications, such as circulators [1–3], isolators [4], tunable phase shifters [5,6], tunable filters [7,8], antennas [9–19], etc. For antenna design, using ferrite materials can obtain bandwidth enhancement [9–15], miniaturization [14–16], pattern reconfiguration [17], and mutual coupling increasing [18,19], etc.

In this paper, we aim at increasing a mobile phone antenna's bandwidth by using Yttrium iron garnet (YIG) ferrite. The general used frequency bands of the second generation (2G), the third generation (3G) and the fourth generation (4G) mobile communication cover 0.698–0.96 and 1.71–2.69 GHz. The lower band of the fifth generation (5G) has been commercially launched in many countries covering 3.3–3.6 and 4.8–5 GHz. To design a mobile phone antenna, conventional techniques mainly focus on geometry modification or lumped circuit design. These techniques include arranging multiple strips on top layers [20], etching multiple slots on ground planes [21] and using the mobile phone's metal rim as a radiator [22] to excite multiple resonances. Lumped capacitances or inductors are adopted to obtain better impedance matching [23]. RF switches [24], PIN diodes [25], and varactor diodes [26] are used to tune current distribution lengths forming frequency reconfigurable antennas. Compared with the aforementioned techniques, adopting ferrite materials to enhance antenna bandwidth has the virtues of simple configuration, easy fabrication, and low cost. Adopting ferrite slab to improve mobile phone antenna's bandwidth has been presented in [14]. The proposed antenna composes of two rectangular slots with a folded shape. With the loading of a ferrite slab, the bandwidth of the antenna in [14] covers 0.667–1.0, 1.09–1.24,1.57–5 GHz.

With the development of the Internet of Things (IoT), many mobile terminals will access 5G communication systems. To save frequency spectrum resources, 2G, 3G and 4G bands are still used in 5G systems. A mobile phone antenna needs to cover 2G, 3G, 4G, and 5G bands which is challenging for antenna design. This paper aims at designing a wideband mobile phone antenna covering 2G, 3G, and 4G bands and the lower band of 5G by using a ferrite slab.

Two antennas of the proposed antenna and a reference antenna were investigated in this paper. A YIG ferrite slab with a size of 15 mm × 15 mm × 2 mm is mounted on the ground plane of each antenna to increase bandwidth. The proposed antenna with the ferrite slab has a wide bandwidth of 0.669–1.533 and 1.69–5 GHz covering the popularly used bands of 2G, 3G, 4G, and the lower band of 5G.

2. Design of Proposed Antenna without Ferrite Slab

Figure 1 shows the configuration of the proposed and reference antennas without a ferrite slab. The two antennas have the same shaped ground plane etched with an open-ended slot as shown in Figure 1a. The top layer of the reference antenna is shown in Figure 1b which derives from our previous work [27]. The reference antenna is fed with a 50 Ω microstrip line connected to a circular patch joined to a rectangular patch. The rectangular patch is split into two parts (Strip1/strip2) with different widths and lengths to increase the bandwidth forming the proposed antenna. The substrates of the two antennas are both 0.8 mm thick FR4 with a relative dielectric constant of 4.4, loss tangent of 0.02, and size of 60 mm × 115 mm. The dimension parameters are w_1 = 1 mm, w_2 = 4 mm, l_2 = 33 mm, g = 2 mm.

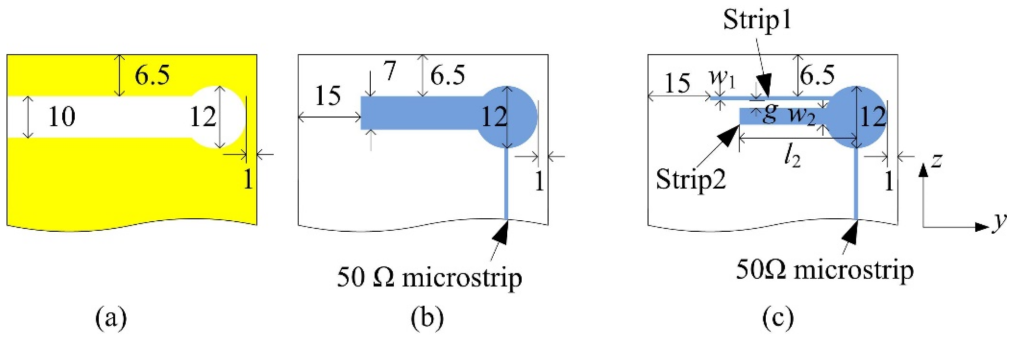

Figure 1. Configuration of the proposed antenna and reference antenna without ferrite slab (unit: mm). (**a**) Bottom layer of the two antennas. (**b**) Top layer of the reference antenna. (**c**) Top layer of the proposed antenna. (Unit: mm).

Figure 2 shows the simulated $|S_{11}|$ plots of the proposed antenna and reference antenna. Simulations are performed using HFSS 15.0. As shown in the figure, the simulated bandwidth of the proposed antenna with $|S_{11}| < -6$ dB is 0.76–1.31 and 2.12–5 GHz, and the one of the reference antenna is 0.78–1.27 and 2.3–5 GHz. Simulation shows that the two antennas have very wide bandwidth at the upper band above 2.4 GHz which owes to the similar shapes of slots and feedings. It is also shown that the proposed antenna has a wider bandwidth than the reference antenna at the lower band. The bandwidth of the proposed antenna needs to be enhanced further to cover the whole bands of 2G, 3G, 4G and the lower band of 5G which will be achieved by using the YIG ferrite slab presented in the following section.

The influences of dimensions of Stip1 and Strip 2 have been investigated. The changes in the dimensions have much influence on $|S_{11}|$ at frequencies below 3 GHz but little at frequencies above 3 GHz. To show the difference between plots clearly, the frequency range drawn in the figures is set to 0.5–3 GHz. As shown in Figure 2, there are two working bands. One is in the frequency range lower than 1.5 GHz and the other one is higher than 1.5 GHz. We call the lower band the first band and the upper band the second band in the following discussion. Figure 3 shows the influence of Strip 1′s width of w_1 on $|S_{11}|$. As shown in the figure, the change of w_1′s value has much influence on $|S_{11}|$ at the second band. In the cases of w_1 = 0.6 mm and w_1 = 0.8 mm, $|S_{11}|$ values are higher than the case of

w_1 = 1 mm. In the case of w_1 = 1.2 mm, $|S_{11}|$ values are higher than −6 dB at frequencies of 2.2–2.4 GHz. Therefore, the optimized value of w_1 is chosen as 1 mm.

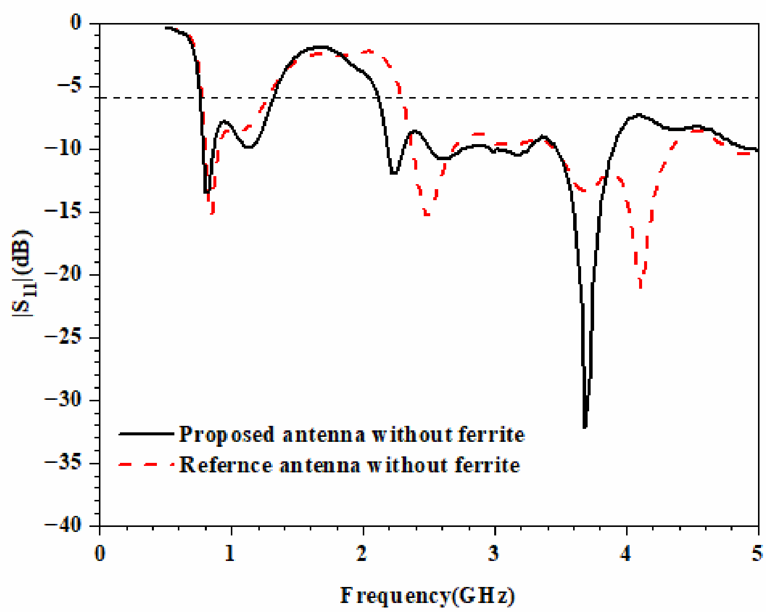

Figure 2. Simulated $|S_{11}|$ of the proposed antenna and the reference antenna without ferrite slab.

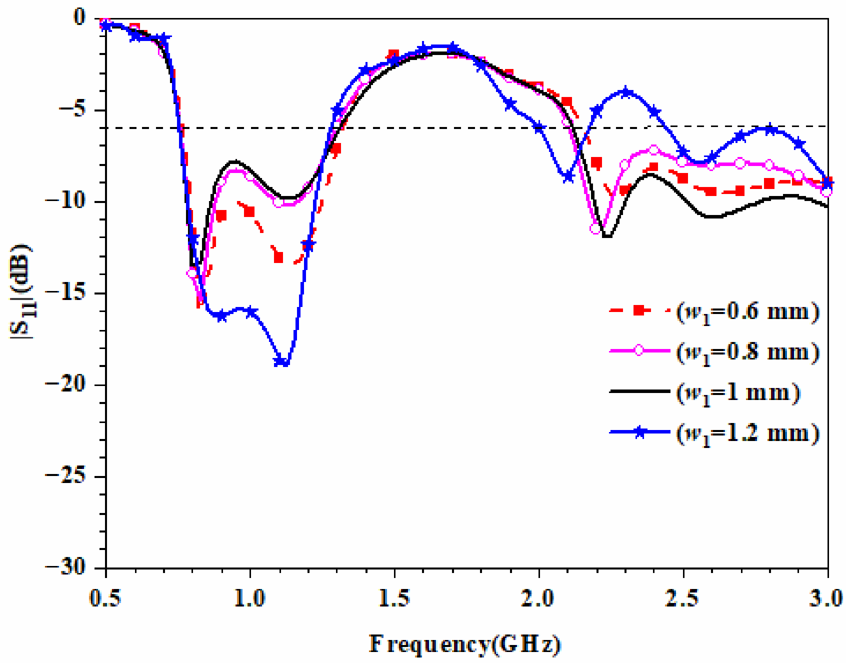

Figure 3. Influence of w_1 on $|S_{11}|$.

Figure 4 shows the influence of Strip 2′s width of w_2 on $|S_{11}|$. As shown in the figure, the change in w_2′s value has much influence on $|S_{11}|$ at the second band. In the cases of w_2 = 2 mm and w_2 = 3 mm, the left cutoff frequencies at the second band are higher than in the case of w_2 = 4 mm. In the case of w_2 = 5 mm, $|S_{11}|$ values are higher than in the case of w_2 = 4 mm at frequencies of 2.2–2.8 GHz. Therefore, the optimized value of w_2 is chosen as 4 mm.

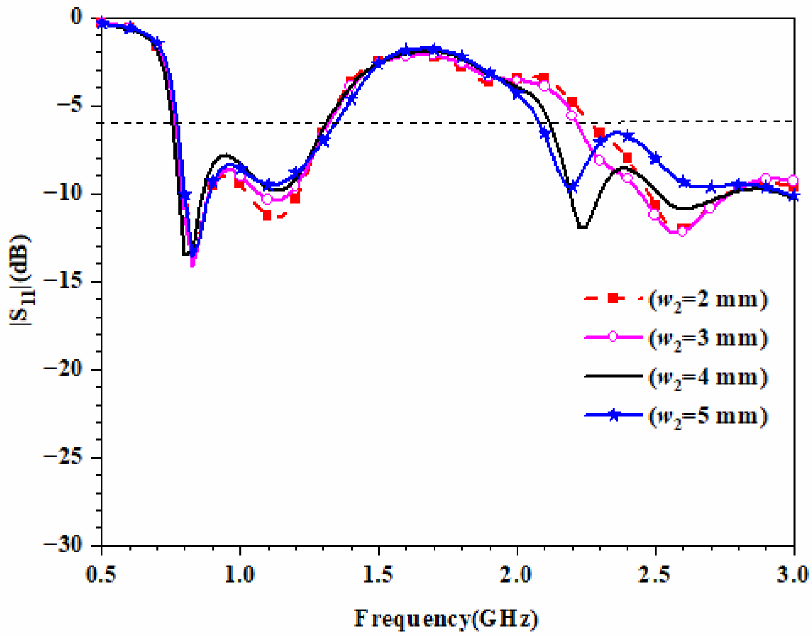

Figure 4. Influence of w_2 on $|S_{11}|$.

Figure 5 shows the influence of Strip 2′s length of l_2 on $|S_{11}|$. As shown in the figure, the change in w_2′s value has much influence on $|S_{11}|$ at the second band. In the cases of l_2 = 29 mm and l_2 = 31 mm, the left cutoff frequencies are larger than in the case of l_2 = 33 mm. In the case of l_2 = 35 mm, $|S_{11}|$ values are higher than −6 dB at frequencies of 2.3–2.4 GHz. Therefore, the optimized value of l_2 is chosen as 33 mm.

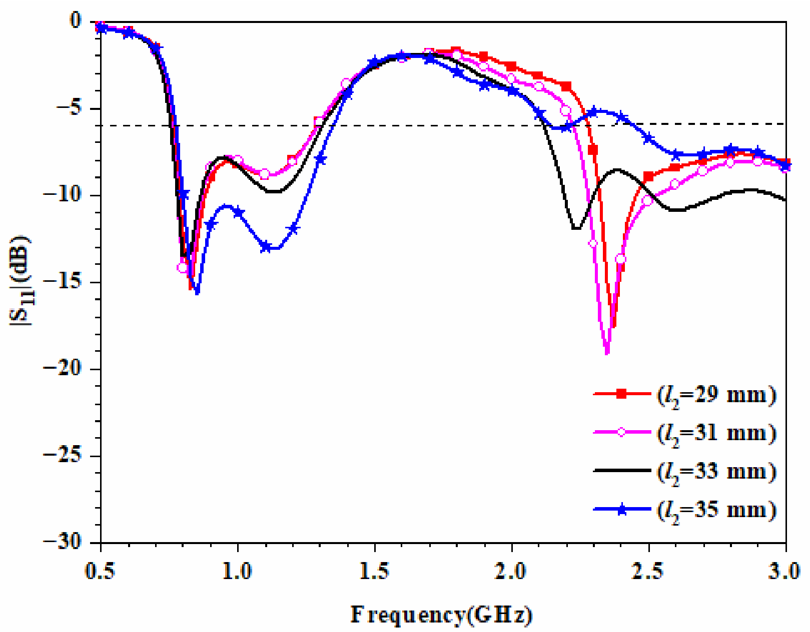

Figure 5. Influence of l_2 on $|S_{11}|$.

Figure 6 shows the influence of the gap between Strip1/Strip2 g on $|S_{11}|$. As shown in the figure, the change in g′s value has much influence on $|S_{11}|$ at the second band. In the cases of g = 0 mm which means that there is no gap between Strip1/Strip2, the left cutoff frequency of the second band is much higher than in the other cases. In the case of g = 1 mm, |S11| values are higher than in the case of g = 2 mm at frequencies of 2.1–3 GHz.

In the case of g = 3 mm, $|S_{11}|$ values are higher than −6 dB at frequencies of 2.2–2.4 GHz. Therefore, the optimized value of g is chosen as 2 mm.

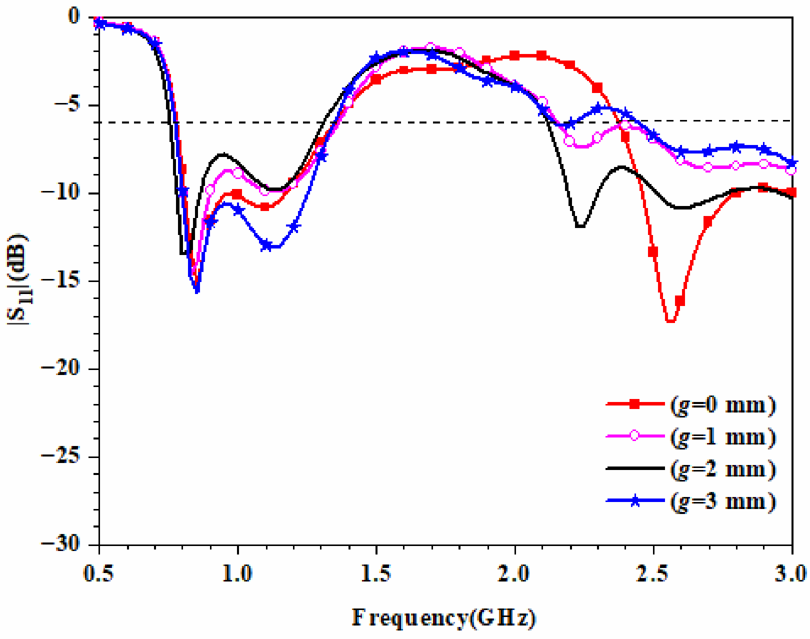

Figure 6. Influence of g on $|S_{11}|$.

3. Design and Measurement of Antennas with Ferrite Slabs

The configuration of the proposed and reference antennas loaded with ferrite slab is shown in Figure 7. The antennas are investigated with the ferrite mounted on the ground plane (shown in Figure 7c) and on the top layer (shown in Figure 7d). Each ferrite slab has a size of 15 mm × 15 mm ×2 mm.

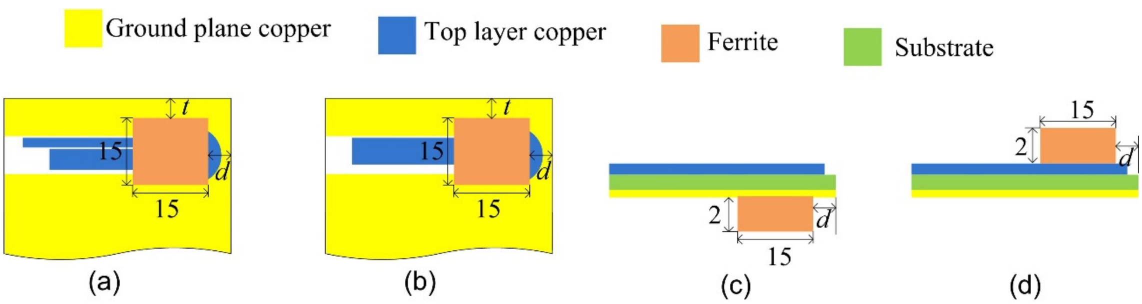

Figure 7. Configuration of the proposed, reference antenna loaded with ferrite slab (unit: mm). (**a**) Top view of the proposed antenna loaded with ferrite slab. (**b**) Top view of the reference antenna with ferrite slab. (**c**) Side view in the case of ferrite slab mounted on the ground plane. (**d**) Side view in the case of ferrite slab mounted on the top layer.

Figure 8 shows the photographs of the fabricated antennas with ferrite slabs on the ground plane at the position of d = 0 mm and t = 2.5 mm for both antennas. Measurement has been conducted by using an Agilent vector network analyzer N5224A which shows that wider bandwidth is obtained when the ferrite slab is arranged around the slot region. Figure 9 shows the measured $|S_{11}|$ plots of the two antennas with and without ferrite slab. As shown in the figure, the measured bandwidth with $|S_{11}| < -6$ dB of the proposed antenna with ferrite slab is enhanced to 0.669–1.533 and 1.69–5 GHz compared with the bandwidth of 0.81–1.44 and 2.3–5 GHz for the antenna without ferrite. The bandwidth of the reference antenna with ferrite slab is enhanced to 0.715–5 GHz compared with the bandwidth of 0.813–1.01, 1.11–1.3 and 2.33–5 GHz for the antenna without ferrite. The loading of the ferrite slab results in wider bandwidths for both antennas. It is also shown that the proposed antenna has a wider bandwidth than the reference one. Furthermore, considering $|S_{11}| < -10$ dB, the measured bandwidth of the proposed antenna with ferrite loading covers 0.71–0.83, 1.87–2.62, 2.99–3.28 and 3.48–5 GHz. Moreover, the bandwidth with $|S_{11}| < -7$ dB covers 0.682–1.49 and 1.76–5 GHz.

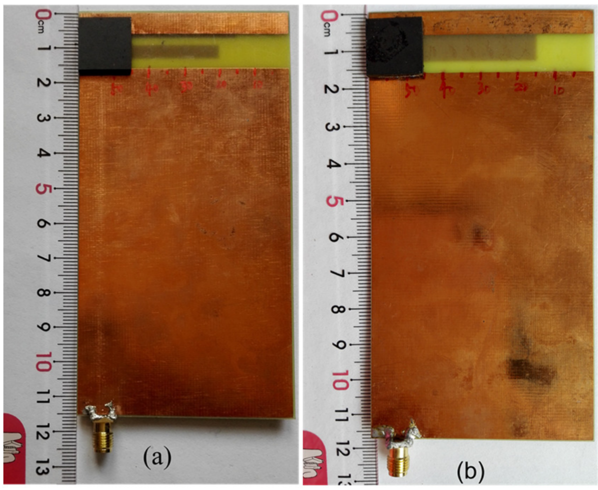

Figure 8. Photograph of the antennas with ferrite slab on bottom layer. (**a**) proposed antenna. (**b**) reference antenna.

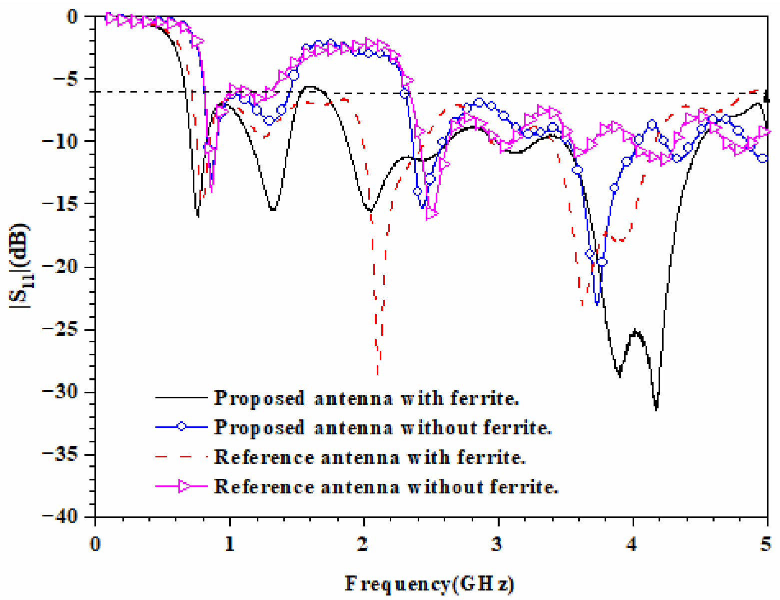

Figure 9. Measured $|S_{11}|$ of the proposed antenna and the reference antenna.

The effects of the ferrite's position on $|S_{11}|$ of the proposed antenna are also investigated. Figure 10 shows the measured $|S_{11}|$ of the proposed antenna with ferrite slab on the ground plane versus the parameters of ferrite's position *d* and *t*. Figure 11 shows the measured $|S_{11}|$ of the proposed antenna with a ferrite slab on the top layer. Table 1 gives the bandwidth of the proposed antenna shown in Figures 10 and 11. As shown in the table, the loading of the ferrite slab at any position results in the frequency band shifting to the lower compared with the case of no ferrite slab loading. The antenna with a ferrite slab on the ground plane has a lower left cutoff frequency than the one with a ferrite slab on the top layer with the same values of parameters *d* and *t*. The proposed antenna has the widest bandwidth when the ferrite slab is loaded on the ground plane covering the circular slot with *d* = 0 mm and *t* = 2.5 mm.

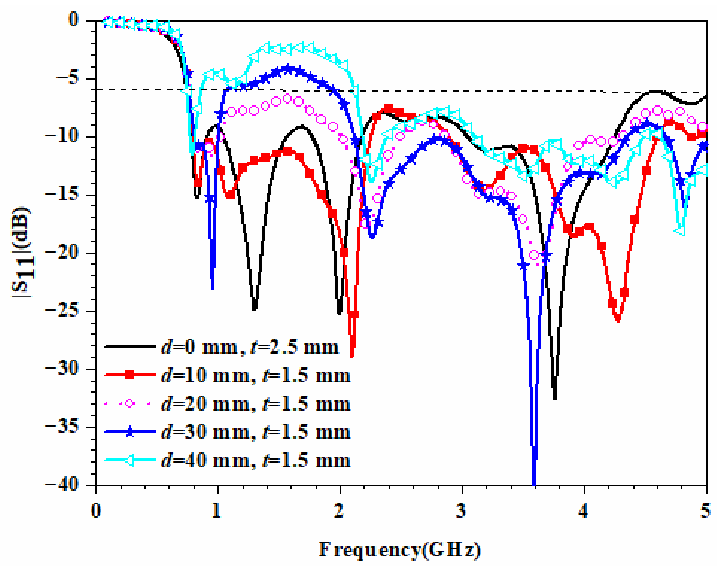

Figure 10. Frequency behavior of measured $|S_{11}|$ of the proposed antenna with ferrite slab on the ground plane versus the ferrite's position.

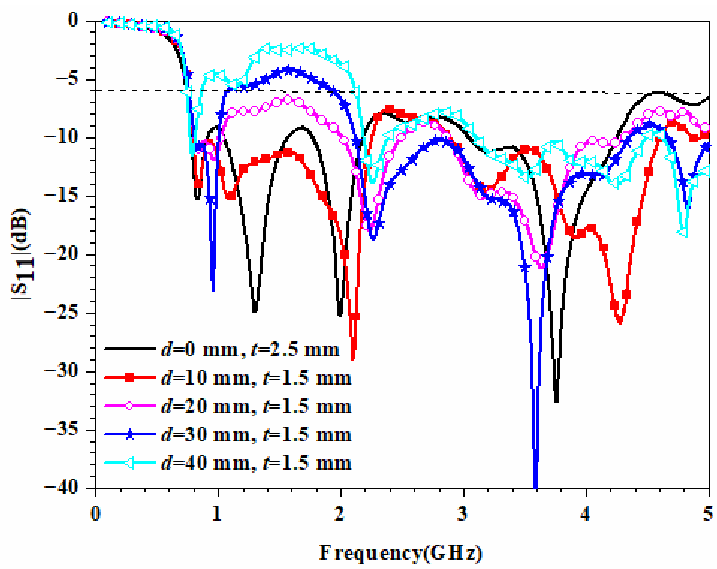

Figure 11. Frequency behavior of measured $|S_{11}|$ of the proposed antenna with ferrite slab on the top layer versus the ferrite's position.

Table 1. Bandwidth of the proposed antenna with ferrite slab mounted on the ground plane and the top layer at different positions.

Ferrite Position (mm)	Bandwidth with Ferrite Slab on the Ground Plane (GHz)	Bandwidth with Ferrite Slab on the Top Layer (GHz)
d = 0, t = 2.5	0.669–1.533, 1.69–5	0.743–5
d = 10, t = 1.5	0.74–5	0.765–5
d = 20, t = 1.5	0.73–5	0.763–5
d = 30, t = 1.5	0.73–0.87, 1.16–1.47	0.764–1.07, 1.94–5
d = 40, t = 1.5	0.73–0.84, 2.19–5	0.746–0.863, 2.12–5
Without Ferrite Slab	0.81–1.44, 2.3–5	

The radiation patterns were measured in a microwave anechoic chamber. The schematic diagram of the radiation pattern measurement setup is illustrated in Figure 12. The system is mainly composed of a vector network analyzer (VNA), a source antenna, and the antenna under test (AUT). The radiation pattern was obtained from transmission coefficients by rotating the AUT. Antenna gain was measured by replacing the AUT with an antenna with standard gain and computed by comparing the transmission coefficients between the AUT and the standard antenna. Figure 13 shows the measured radiation pattern in the *x*-*y*, *x*-*z*, and *y*-*z* planes at 0.787 GHz, 0.88 GHz, 2.17 GHz, and 2.4 GHz, respectively. The patterns are near-omnidirectional. The maximum gains at the four frequencies are 0.17 dBi, 2 dBi, −2.91 dBi, and −0.93 dBi, respectively. The antenna meets the directional requirement of mobile phones.

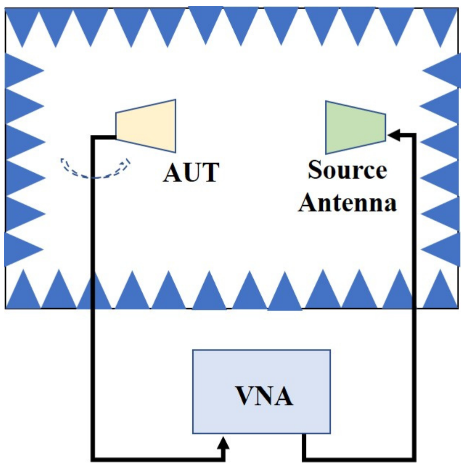

Figure 12. Schematic diagram of radiation pattern measurement setup.

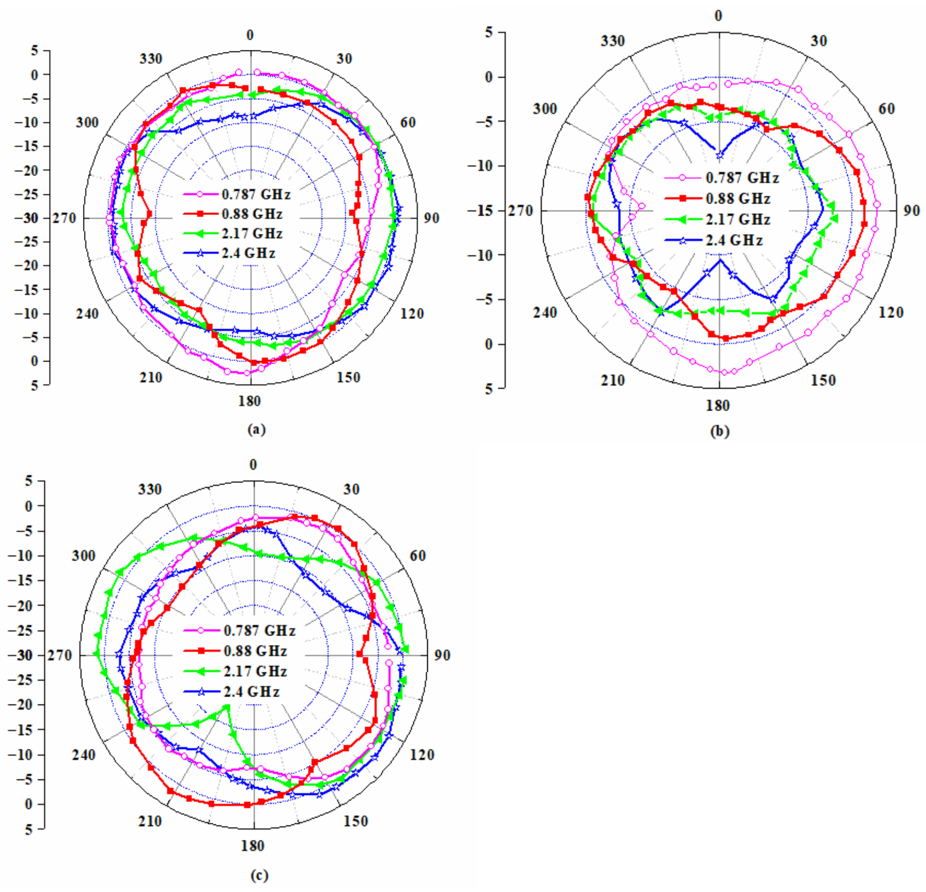

Figure 13. Measured radiation patter. (**a**) *x*-*y* plane. (**b**) *x*-*z* plane. (**c**) *y*-*z* plane.

A comparison of the proposed antenna with antennas in published literature is given in Table 2. As shown in the table, the proposed antenna has a wider bandwidth than the published ones.

Table 2. Comparison of the proposed antenna with antennas in published literatures.

Reference	Antenna Dimension (mm^3)	Antenna Type	Bandwidth (GHz)	Gain	Efficiency
[11]	52 × 8 × 3	Helix	0.173–0.202	NA	NA
[12]	18 × 8 × 3	monopole	0.698–0.751, 1.656–2.171	>−1.67	>33%
[13]	35 × 15 × 4	monopole	0.745–0.973, 1.536–2.825	NA	>47%
[14]	59 × 14 × 2.8	slot	0.667–1.0, 1.09–1.24, 1.57–5	NA	NA
Proposed	59 × 12 × 2.8	slot	0.669–1.533, 1.69–5	>−2.93	NA

4. Conclusions

A novel technique to enhance the bandwidth of mobile phone antenna is proposed by loading a ferrite slab on the ground plane. The technique was validated using a novel slot antenna. The ferrite slab locates around the slot region with a small area of 15 mm × 15 mm and an acceptable height of 2 mm. The measured bandwidth of the proposed antenna with ferrite slab is enhanced to 0.669–1.533 and 1.69–5 GHz compared with the bandwidth of 0.81–1.44 and 2.3–5 GHz for the antenna without ferrite. The mounting of the ferrite slab obtains significant bandwidth enhancement. Compared with conventional miniaturized mobile phone antennas, the proposed antenna loaded with ferrite has a simpler configuration and a wider bandwidth. The bandwidth of the proposed antenna covers the popularly used bands of 2G, 3G, 4G and the lower band of 5G. The radiation performance of the proposed antenna satisfies the requirements of a mobile phone.

Author Contributions: Simulation, data plotting and ferrite material, P.L.; writing, simulation, fabrication, W.-H.Z.; fabrication and measurement guide, Z.J.; radiation pattern measurement, Z.Y., X.Q.; ferrite material, S.L. All authors have read and agreed to the published version of the manuscript.

Funding: This work was supported by the Natural Science Foundation of Shandong Province, China (Grant No. ZR2020MF023).

Institutional Review Board Statement: Not applicable.

Informed Consent Statement: Not applicable.

Data Availability Statement: Not applicable.

Conflicts of Interest: The authors declare no conflict of interest.

References

1. Afshani, A.; Wu, K. Generalized theory of concurrent multimode reciprocal and, or nonreciprocal SIW ferrite devices. *IEEE Trans. Microwa. Theory Techn.* **2021**, *69*, 4406–4421. [CrossRef]
2. Olivier, V.; Monediere, T.; Lenoir, B.; Turli, H.; Breuil, C.; Pouliguen, P.; Huitema, L. General coupling method for stripline ferrite circulators: Application on dual-band devices with complex central conductor shape. *IEEE Trans. Microwa. Theory Techn.* **2022**, *70*, 3486–3497. [CrossRef]
3. Ren, H.; Xie, Y.; Wei, H.; Wu, P.; Dai, L. A novel circulator construction with high multipactor threshold and high isolation for aerospace applications. *IEEE Trans. Plasma Sci.* **2022**, *50*, 715–720. [CrossRef]
4. Noferesti, M.; Djerafi, T. A tunable ferrite isolator for 30 GHz millimeter-wave applications. *IEEE Trans. Magn.* **2021**, *57*, 1–7. [CrossRef]
5. Nafe, A.; Shamim, A. An integrable SIW phase shifter in a partially magnetized ferrite LTCC package. *IEEE Trans. Microwa. Theory Techn.* **2015**, *63*, 2264–2274. [CrossRef]
6. Yang, G.; Sun, N.X. Tunable ultrawideband phase shifters with magnetodielectric disturber controlled by a piezoelectric transducer. *IEEE Trans. Magn.* **2014**, *50*, 1–4. [CrossRef]
7. Du, S.; Yang, Q.; Wang, M.; Fan, X. A magnetically tunable bandpass filter with high out-of-band suppression. *IEEE Trans. Magn.* **2022**, *58*, 1–5. [CrossRef]
8. Kagita, S.; Basu, A.; Koul, S.K. Characterization of LTCC-based ferrite tape in X-band and its application to electrically tunable phase shifter and notch filter. *IEEE Trans. Magn.* **2017**, *53*, 1–8. [CrossRef]

9. Hasan, I.H.; Hamidon, M.N.; Ismail, A.; Ismail, I.; Mekki, A.S.; Kusaimi, M.A.M.; Azhari, S.; Osman, R. YIG thick film as substrate overlay for bandwidth enhancement of microstrip patch antenna. *IEEE Access* **2018**, *6*, 32601–32611. [CrossRef]
10. Wang, B.; Yang, S.; Zhang, Z.; Chen, Y.; Qu, S.; Hu, J. A ferrite-loaded ultralow profile ultrawideband tightly coupled dipole array. *IEEE Trans. Antennas Propag.* **2022**, *70*, 1965–1975. [CrossRef]
11. Xia, Q.; Su, H.; Zhang, T.; Li, J.; Shen, G.; Zhang, H.; Tang, X. Miniaturized terrestrial digital media broadcasting antenna based on low loss magneto-dielectric materials for mobile handset applications. *J. Appl. Physics.* **2012**, *112*, 043915. [CrossRef]
12. Cheon, Y.; Lee, J.; Lee, J. Quad-band monopole antenna including LTE 700MHz with magneto-dielectric material. *IEEE Antennas Wirel. Propag. Lett.* **2012**, *11*, 137–140. [CrossRef]
13. Park, B.-Y.; Jeong, M.-H.; Park, S.-O. A magneto-dielectric handset antenna for LTE, WWAN, GPS applications. *IEEE Antennas Wirel. Propag. Lett.* **2014**, *13*, 1482–1485. [CrossRef]
14. Meng, Y.; Xiao, X.; Zong, W.-H.; Huang, Q.-Y.; Li, S.; Wang, J. A wideband antenna loaded with ferrite for mobile phone applications. In Proceedings of the International Applied Computational Electromagnetics Society Symposium, Suzhou, China, 1–4 August 2017; IEEE: New York, NY, USA.
15. Shi, J.; Liu, H.; Wang, X.; Zhang, J.; Han, F.; Tang, X.; Wang, J. Miniaturized dual-resonant helix, spiral antenna system at MHz-band for FSK impulse radio intrabody communications. *IEEE Trans. Antennas Propag.* **2020**, *68*, 6566–6579. [CrossRef]
16. Gu, W.; Luong, K.; Yao, Z.; Cui, H.; Wang, Y.E. Ferromagnetic resonance-enhanced electrically small antennas. *IEEE Trans. Antennas Propag.* **2021**, *69*, 8304–8314. [CrossRef]
17. Shirkolaei, M.M.; Ghalibafan, J. Scannable leaky-wave antenna based on ferrite-blade waveguide operated below the cutoff frequency. *IEEE Trans. Magn.* **2021**, *57*, 1–10. [CrossRef]
18. Zhu, J.; Xie, S.; Jin, C.; Liu, X.; Liu, H. Strategies for a high sensitivity ferrite-core RFID tag antenna using in oil well downhole applications. *IEEE Trans. Magn.* **2022**, *58*, 1–5. [CrossRef]
19. Zhu, J.; Jin, C.; Liu, H. Mutual inductance modeling of two coaxial solenoid antennas with large ferrite core for underground RFID applications. *IEEE Trans. Magn.* **2021**, *57*, 1–4. [CrossRef]
20. Huang, D.; Du, Z.; Wang, Y. An octa-band monopole antenna with a small nonground portion height for LTE, WLAN mobile phones. *IEEE Trans. Antennas Propagat.* **2017**, *65*, 878–882. [CrossRef]
21. Deng, C.; Li, Y.; Zhang, Z.; Feng, Z. Planar printed multi-resonant antenna for octa-band WWAN, LTE mobile handset. *IEEE Antennas Wirel. Propagat.* **2015**, *14*, 1734–1737. [CrossRef]
22. Yang, Y.; Zhao, Z.; Yang, W.; Nie, Z.; Liu, Q.-H. Compact multimode monopole antenna for metal-rimmed mobile phones. *IEEE Trans. Antennas Propagat.* **2017**, *65*, 2297–2304. [CrossRef]
23. Chen, H.; Zhao, A. LTE antenna design for mobile phone with metal frame. *IEEE Antennas Wirel. Propagat.* **2016**, *15*, 1462–1465. [CrossRef]
24. Lee, W.-W.; Hong, S. A multiband and wideband antenna using RF switch for mobile application. *Microw. Opt. Technol. Lett.* **2015**, *57*, 1491–1494. [CrossRef]
25. Lee, S.W.; Sung, Y. Compact frequency reconfigurable antenna for LTE, WWAN mobile handset applications. *IEEE Trans. Antennas Propagat.* **2015**, *63*, 4572–4577. [CrossRef]
26. Stanley, M.; Huang, Y.; Wang, H.; Zhou, H.; Tian, Z.; Xu, Q. A novel reconfigurable metal rim integrated open slot antenna for octa-band smartphone applications. *IEEE Trans. Antennas Propag.* **2017**, *65*, 3352–3363. [CrossRef]
27. Zong, W.-H.; Yang, X.-M.; Li, S.-D.; Wei, X.-Y.; Hou, J.-C. Design and fabrication of a wideband slot antenna for handset applications. In Proceedings of the 2015 IEEE International RF and Microwave Conference, Kuching, Malaysia, 14–16 December 2015; pp. 161–165.